Journal of Magnetism and Magnetic Materials 322 (2010) 443–447

Contents lists available at ScienceDirect

Journal of Magnetism and Magnetic Materials

journal homepage: www.elsevier.com/locate/jmmm

Effects of electron correlation and spin–orbit coupling on the electronic and magnetic properties of $TbCu_3Mn_4O_{12}$

X.J. Liu [a,b], J. Meng [a], E. Pan [b,*], J.D. Albrecht [c]

[a] State Key Laboratory of Rare Earth Resources Utilization, Changchun Institute of Applied Chemistry, Chinese Academy of Sciences, PR China 130022
[b] Computer Modeling and Simulation Group, College of Engineering, University of Akron, Ohio 44325-3905, USA
[c] Air Force Research Laboratory, Wright-Patterson Air Force Base, Ohio 45433, USA

ARTICLE INFO

Article history:
Received 18 August 2009
Received in revised form
15 September 2009
Available online 1 October 2009

Keywords:
Three magnetic-sublattice perovskite
Electronic correlation and spin-orbit coupling effect
Electronic correlation effect
Spin-orbit coupling effect

ABSTRACT

Electronic and magnetic properties of the three magnetic-sublattice double perovskite $TbCu_3Mn_4O_{12}$ (TCMO) are investigated by performing first-principles density-functional theory calculations. Our electronic structure calculations show that TCMO is half-metallic and its half-metallicity can only be correctly described when the electron correlation on Tb^{3+} $4f^8$ electrons are considered. The energies of different magnetic configurations among the three magnetic sublattices are also calculated, revealing that the magnetic configuration with Mn and Cu spins in the antiparallel arrangement and with the Tb magnetic moments ferromagnetically/antiferromagnetically (FM/AFM) coupled to Cu/Mn spins (that is $Tb^{\downarrow}Cu_3^{\downarrow}Mn_4^{\uparrow}O_{12}$) is the lowest energetic magnetic state, which is consistent with recent experimental results. The magnetic anisotropy is further calculated for the [1 1 1], [1 1 0], and [0 0 1] spin quantization directions. It is found that the [1 1 1]-direction is more stable than the [1 1 0]- and [0 0 1]-directions by 123 and 135 meV per formula unit, respectively, indicating a significant magnetic anisotropy. Our detailed projected partial density of states analysis finally shows that Cu and Mn are antiferromagnetically coupled by superexchange interaction and Tb is expected to interact FM with A-site Cu and AFM with B-site Mn sublattices by way of *4f*–2*p*–3*d*.

1. Introduction

Perovskite transition-metal oxides have been intensively studied due to their range of intriguing physical properties [1]. These include ferroelectricity, complex charge, spin and/or orbital order, and even some combined properties such as multiferroicity [2] and colossal magnetoresistance [3]. Recently, the complex perovskite $CaCu_3Mn_4O_{12}$ has attracted great attention as a potential candidate as a colossal magnetoresistance material [4–7]. As is well known, there are two methods to tailor the properties of perovskite materials: B-site substitution and carrier doping. While the former modifies the band structure, the latter mainly shifts the Fermi level. Substituting Ca^{2+} by R^{3+} (trivalent rare-earth ions) belongs to the latter method. In this system, such a substitution induces electron doping in B-site Mn ions which then affects the magnetic and transport properties, as demonstrated for R=La, Ce, Nd, Th and Tb [7–10].

It has also been found that $CaCu_3Mn_4O_{12}$ is a semiconductor with states energetically below the Fermi level which exhibit a strong Cu *d* character and states above the Fermi level with a strong Mn *d* character [11,12]. If one replaces Ca^{2+} by R^{3+}, the electron-doping effect would lead to the occurrence of a mixed Mn^{4+}–Mn^{3+} valence at the B sublattice. Consequently, the additional valence electrons present upon replacement of Ca^{2+} by R^{3+} would be concomitant with some density of states across the Fermi level and thus result in half-metallicity. This hypothesis has been verified by our accurate full-potential density-functional theory calculation of $LaCu_3Mn_4O_{12}$ [11].

Recently, a new family of ferromagnetic materials with three magnetic sublattices has been discovered [13,14]. These materials have proven to be not only fundamentally interesting, but also technologically important [15], inspiring the search for new promising magnetic compounds. Since most rare-earth ions (R^{3+}) are also magnetic, $RCu_3Mn_4O_{12}$ can be a three-sublattice magnetic system with potential ferromagnetic-type ordering. Therefore, it is of particular interest to examine the effect of the electron correlation effect on the electronic and magnetic properties of the three-sublattice magnetic perovskite systems. In addition, to the best of our knowledge, there is no existing investigation on the magnetic coupling among the three magnetic sublattices from first-principles, especially when the *4f* electrons are included.

In this paper, we therefore investigate the electronic and magnetic properties of the three magnetic-sublattice double

* Corresponding author.
E-mail addresses: jmeng@ciac.jl.cn (J. Meng), pan2@uakron.edu (E. Pan).

0304-8853/$ - see front matter © 2009 Elsevier B.V. All rights reserved.
doi:10.1016/j.jmmm.2009.09.073

perovskite $TbCu_3Mn_4O_{12}$ (TCMO) by performing first-principles density-functional theory calculations. The calculated electronic structures show that TCMO is half-metallic and its half-metallicity can only be correctly described when the electron correlation on Tb^{3+} $4f^8$ electrons are considered. The computed energies for different magnetic configurations among the three magnetic sublattices reveal that the magnetic configuration with Mn and Cu spins in the antiparallel arrangement and with the Tb magnetic moments ferromagnetically/antiferromagnetically (FM/AFM) coupled to Cu/Mn spins (that is $Tb^{\downarrow}Cu_3^{\downarrow}Mn_4^{\uparrow}O_{12}$) is the lowest energetic magnetic state, which is consistent with recent experimental results. The magnetic anisotropy by taking into account spin–orbit coupling effect is further calculated for the [111], [110], and [001] spin quantization directions. It is found that the [111]-direction is more stable than the [110]- and [001]-directions by 123 and 135 meV per formula unit, respectively, indicating a significant magnetic anisotropy. Our detailed projected partial density of states analysis finally shows that Tb is expected to interact ferromagnetically with A-site Cu and antiferromagnetically with B-site Mn sublattices by way of 4*f*–2*p*–3*d*.

The rest of paper is organized as follows. In Section 2, the theoretical method is briefly outlined and the computational details are presented. In Section 3, we present the calculated results and discuss the electronic and magnetic properties of this special material. Conclusions are drawn in Section 4.

2. Computational details

First-principles DFT electronic structure calculations were performed using the full-potential augmented plane wave plus local orbital method as implemented in the WIEN2K code [16]. Non-overlapping muffin-tin sphere radii of 2.50, 1.94, 1.91 and 1.68 a.u. were used for the Tb, Cu, Mn and O atoms, respectively. The expansion in the spherical harmonics of the radial wave functions was taken up to order $l=10$. The value of $R_{MT}^{\min}K_{\max}$ (the product of the smallest atomic sphere radii R_{MT} and the plane-wave cutoff parameter $K_{\max}$) was set to be 7.0. The total Brillouin zone was sampled with 1000 *k* points. The exchange-correlation energy functional was incorporated using the generalized gradient approximation (GGA) [17]. The SOC was included in the calculations based on the second variational approach [18–20] using a basis set of states up to 60 eV above the Fermi energy. In WIEN2K [16], core states are treated fully relativistically whilst for valence states relativistic effects are included either in a scalar-relativistic treatment or with the second variational method including spin–orbit coupling. The calculation including SOC is based on the scalar-relativistic wavefunctions. Thus, our calculation is fully relativistic when SOC is considered. In addition, the electron correlation in the 4*f* electrons (as well as in Cu 3*d* electrons) was considered using the GGA plus on-site repulsion U method [21–23] with the effective *U* values ($U_{eff}=U-J$) as follows: the GGA+U_f calculation was carried out with $U_{eff}=0.44$ Ry (6.0 eV) for Tb, and GGA+$U_{f,d}$+SOC with $U_{eff}=6.0$ eV for Tb and 5.0 eV for Cu atoms, respectively. Actually, we have carried out a series of calculations from 5 to 12 eV for U_f and from 5 to 7.0 eV for U_d (for Cu 3*d*) and found that the total characters of the electronic structure changed only slightly for different *U*, accompanying with a little energy shift in the occupied and unoccupied orbitals. The self-consistent calculations were considered to be converged when the energy convergence is less than 10^{-5} Ry. The structure parameters of TCMO were taken from the experimental values [12], which are shown in Fig. 1 along with the magnetic coupling among the magnetic ions.

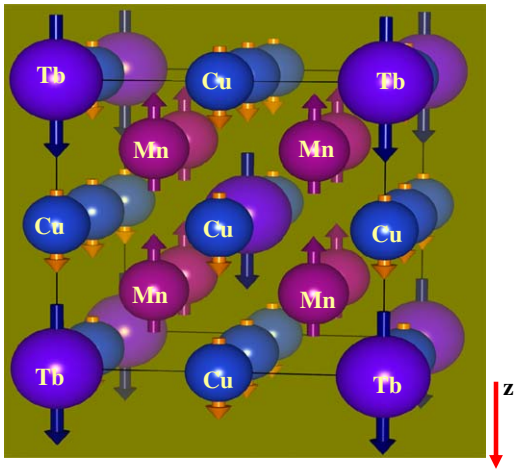

Fig. 1. (Color online) Atomic arrangement and magnetic configuration. The oxygen atoms have been omitted for clarity.

3. Results and discussion

3.1. Magnetic properties in the three magnetic sublattice double perovskite

Although several families with three magnetic sublattice ferrimagnets have been found, there is no theoretical investigation on the coupling among different magnetic ions in them. Therefore, we first design several magnetic arrangements: **FM** (all the magnetic ions are ferromagnetically arranged, as $Tb^{\uparrow}Cu_3^{\uparrow}Mn_4^{\uparrow}O_{12}$), **AF1** (Cu and Mn are antiparallel and Tb is antiferromagnetically/ferromagnetically coupled with Cu/Mn, as $Tb^{\uparrow}Cu_3^{\downarrow}Mn_4^{\uparrow}O_{12}$), and **AF2** (Cu and Mn are antiparallel and Tb ferromagnetically/antiferromagnetically coupled with Cu/Mn, as $Tb^{\downarrow}Cu_3^{\downarrow}Mn_4^{\uparrow}O_{12}$). Although the FM is experimentally inaccessible, it provides a useful reference for understanding the magnetic coupling in this perovskite. We find that the AF2 is the lowest energy state, by about 20 and 1065 meV lower than AF1 and FM, respectively, and that the difference between AF1 and FM is about 1045 meV. The large energy difference between FM and AF1 indicates a strong AFM coupling between Cu and Mn. By assuming a near-neighbor spin Hamiltonian with a Cu–Mn coupling (at the same time neglecting the Tb magnetic coupling between them), we obtained the exchange coupling of $J^{\text{Cu-Mn}}\approx 22$ meV.

Using the same method, we and Pickett evaluated the AFM coupling of Cu–Mn in $CaCu_3Mn_4O_{12}$ to be ~20 meV [11,24]. Thus, it can be seen that the Cu–Mn coupling in $TbCu_3Mn_4O_{12}$ is stronger than that in $CaCu_3Mn_4O_{12}$, which is consistent with the experimental results (T_c is 395 K for $TbCu_3Mn_4O_{12}$ and 355 K for $CaCu_3Mn_4O_{12}$). This result is thought to be a consequence of the increased electron number upon Ca^{2+} replacement by Tb^{3+} that induces a mixed valence state at the Mn sublattice and reinforces the superexchange interactions between Mn and Cu cations. Similarly, from the energy difference between AF1 and AF2, one can see the strength of the magnetic coupling between Tb and Cu (and/or Mn). The energy difference between AF1 and AF2 is only 20 meV, i.e., almost 2 orders of magnitude smaller than the AFM interaction between Cu and Mn (1045 meV between AF1 and FM or 1065 meV between AF2 and FM).

These calculations are consistent with the experimental observation that only below 100 K do the Tb magnetic moments begin to participate in the magnetic ordering while the T_c of Cu and Mn is above room temperature (395 K). Since the AF2 is the most stable magnetic state, we will concentrate our study on this configuration in the following sections.

3.2. Electron correlation and spin–orbit coupling effects on the electronic structures

The spin-polarized GGA calculated total density of states (TDOS) with 4*f* partial density of states (PDOS) (which is shadowed in blue) is presented in Fig. 2(a). It is observed from this figure that metallic behavior is present for the spin-up channel, while for the spin-down channel, an energy gap of 0.40 eV is seen clearly. This suggests that $TbCu_3Mn_4O_{12}$ is a half-metallic compound. At the Fermi level the thermally induced current is 100% spin polarized, which is the unique feature for the half-metallic compounds.

As for the Tb 4*f* orbitals, the bond valence sum calculations showed that the oxidation states of Tb is 3.23 [12]. Thus, the terbium oxidation state is close to +3, which means the *f*-electron counts f^8 (that is $f^{7\downarrow}f^{1\uparrow}$, depends on our definition of the magnetic coupling direction as shown above). The PDOS of 4*f* in Fig. 2(a) further indicates that the occupied spin-down states are positioned below −4.0 eV, while the unoccupied spin-up states are positioned at the Fermi level. The overall width of the 4*f* band (for both spin-up and spin-down) is narrow (approximately 1 eV). Because the bandwidth is small compared to the on-site repulsion *U* (approximately 5–7 eV), it is suspected that electron correlation is important in $TbCu_3Mn_4O_{12}$. The failure of the traditional DFT in describing strongly correlated systems is currently remedied by the DFT plus on-site repulsion-U method. Thus, we employed the GGA+U_f method to see if the 4*f* orbital of Tb can be correctly described using this method.

The TDOS along with PDOS of 4*f* orbitals of Tb for the AF2 state using the GGA+U_f method with U_{eff}=6.0 eV under the experimental crystal structure symmetry Im-3 is shown in Fig. 2(b), which reveals an *f* band splitting in the spin-up channel: one is pushed up to higher energy (around 2.0 eV), the other is still positioned at the Fermi level; while in the spin-down channel the *f* band is shifted from −4.0 eV to a lower energy, −9.0 eV, with no band splitting. Our GGA+U_f calculations with larger U_f values (up to 0.88 Ry, which is 12 eV) did not change the general picture described above, except that the *f* orbitals are tend to shift towards lower and higher energies for the occupied and unoccupied orbitals, respectively, while still keeping some states crossing the Fermi level.

In order to investigate its large anisotropic character of this compound, we also performed GGA+SOC calculations. Fig. 2(c) shows the corresponding results obtained using the GGA+SOC method with the spin quantization taken along the [111]-direction. Both the spin-up and spin-down *f* bands are more dispersed, overlapping with each other, but still retaining some states at the Fermi level for the spin-up channel. We also carried out GGA+SOC calculation with spin quantization taken along the [110]- and [001]-directions. The calculated results for the AF2 state using the GGA, GGA+U_f, GGA+SOC methods are summarized in Table 1. It is shown that the SOC effect makes the system more stable by 1644, 1632 and 1767 meV with the [001]-, [110]- and [111]-directions of quantization, respectively. In particular, the [111]-direction quantization is more stable than those with the [110]- and [001]-directions by 123 and 135 meV per formula unit, respectively, indicating that the easy magnetization axis is along the ternary [111] axis, which is consistent with the experiments [25]. Furthermore, the large energy difference between different spin quantizations indicates that $TbCu_3Mn_4O_{12}$ has significant anisotropic magnetic character.

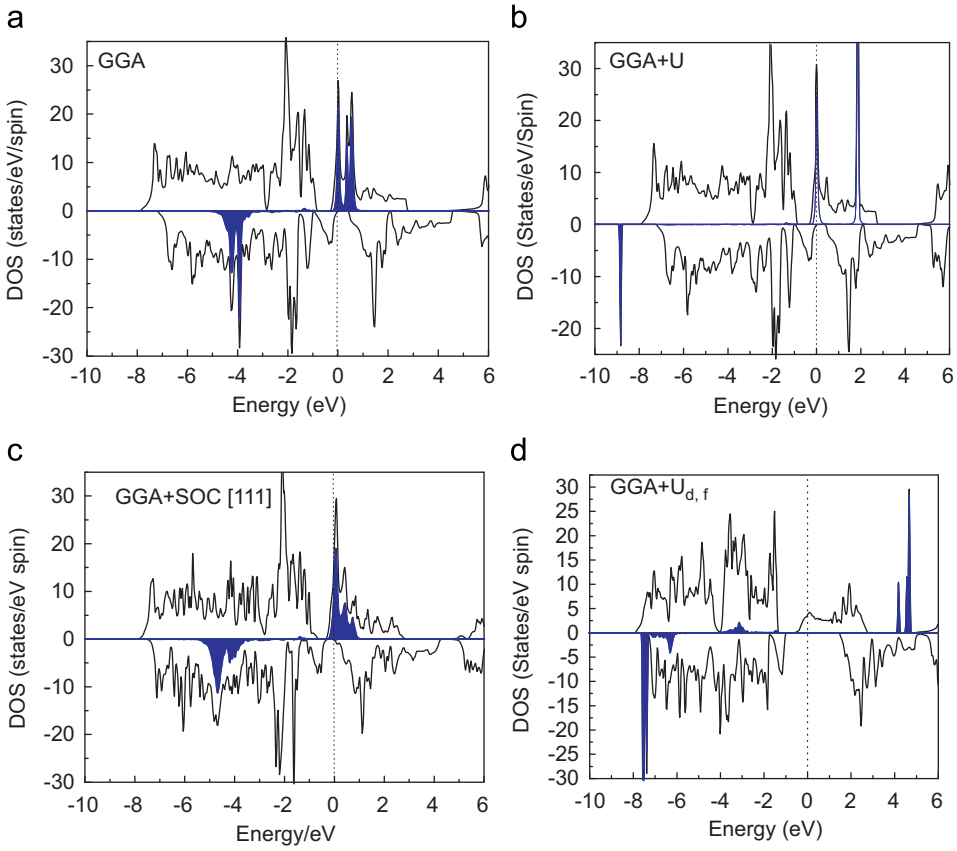

Fig. 2. (Color online) Total density of states (TDOS) along with partial density of states (PDOS) of 4*f* orbitals calculated for $TbCu_3Mn_4O_{12}$ in the AF2 magnetic state using different methods. (a) GGA, (b) GGA+U_f with U_f 6.0 eV under high symmetry, (c) GGA+SOC [111], (d) GGA+$U_{f,d}$ with U_f=6.0 eV U_d=5.0 eV under lower symmetry. The Fermi energy is indicated by the dotted line. The positive and negative values indicate spin up and spin down, respectively.

Table 1
Energy differences and magnetic moments of $TbCu_3Mn_4O_{12}$ (per formula unit), net spin and/or orbital moments of Tb, Cu and Mn (per atom) obtained from GGA, GGA+U_f, GGA+SOC and GGA+U_f+SOC calculations for the lowest magnetic state (that is $Tb^{\downarrow}Cu_3^{\downarrow}Mn_4^{\uparrow}O_{12}$), compared to experimental results.

	GGA	GGA+U_f[a]	GGA+SOC [111]	GGA+SOC [0 0 1][c]	GGA+SOC [1 1 0][e]
ΔE_{total} (meV)	0	–	−1767	−1644	−1632
M_{Tb} (μ_B)	−5.97	−6.20	−5.93	−5.89	−5.90
M_{Cu} (μ_B)	−0.43	−0.42	−0.41	−0.43[d]	−0.43[f]
M_{Mn1} (μ_B)	2.68	2.71	2.65[b]	−0.43	−0.43
M_{Mn2} (μ_B)	4.00	4.00	2.65	−0.43	−0.43
M_{total} (μ_B)			4.08	2.67	2.67[g]
				4.06	2.68
					4.00
	GGA+U_f+SOC [111][h]	GGA+$U_{f,d}$+SOC [111][j]	GGA+$U_{f,d}$[k]	Exp.[12]	
M_{Tb} (μ_B)	−5.97 (−1.84)[i]	−5.98 (−1.97)	−5.99	−5.07	
M_{Cu} (μ_B)	−0.43	−0.71	−0.69	−0.75	
M_{Mn1} (μ_B)	2.64	2.64[b]	3.08	2.59	
M_{Mn2} (μ_B)	2.64	2.64	3.06		
M_{total} (μ_B)	4.00	4.01	4.00		

[a] U_{eff}=6.0 eV for Tb 4*f*.
[b] SOC calculations with [1 1 1]-orientation inducing two different Mn sites.
[c] SOC in [0 0 1]-direction.
[d] SOC calculations with [0 0 1]-orientation inducing three different Cu sites.
[e] SOC in [1 1 0]-direction.
[f] SOC calculations with [1 1 0]-orientation inducing three different Cu sites.
[g] SOC calculations with [1 1 0]-orientation inducing two different Mn sites.
[h] SOC in [1 1 1]-direction with U and SOC being considered on Tb 4*f* orbit.
[i] The orbital moments on Tb atom obtained from the calculation with SOC are given in parentheses.
[j] Both *U* and SOC are considered on Tb 4*f* orbit; simultaneously, *U* is also added to Cu 3*d* orbit.
[k] GGA+$U_{f,d}$ calculation under lower symmetry.

We noticed that the electronic correlation make the electrons of Tb 4*f* localize and SOC breaks the symmetry, relieves the degeneracy and allows these states to split. Therefore, we expect that under lower symmetry, electronic correlation effect can split the Tb 4*f* orbitals on the Fermi level. The calculated TDOS and PDOS of the 4*f* orbitals of Tb are presented in Fig. 2(d), which shows that $TbCu_3Mn_4O_{12}$ is half-metallic with the fully occupied spin-down *f* states around −7.0 eV and partially occupied spin-up *f* states being completely split. The occupied spin-up *f* states are positioned around −3.0 eV below the Fermi level and the unoccupied spin-up 4*f* states are positioned at 4.5 eV above the Fermi level. This phenomenon is reasonable since the 4*f* electrons in $TbCu_3Mn_4O_{12}$ are localized and thus do not affect the valence states near the Fermi level.

Based on the GGA+U_f+SOC calculation, we predicted a spin magnetic moment of Tb being −5.98 μ_B. We also noticed that SOC could induce an unquenched orbital moment as large as −1.84 μ_B on Tb 4*f* orbital (see Table 1). Thus, according to Hund's third rule the total magnetic moment is −7.82 μ_B, which is consistent with other calculations [26]. In addition, the calculated values are larger compared with the measured moment (∼5.07 μ_B) determined from the Neutron Powder Diffraction (NPD) magnetization study of $TbCu_3Mn_4O_{12}$ [12]. This discrepancy can be explained in part by the fact that the zero-field moments were measured at 2 K, but our calculations were carried out under the 0 K condition. In addition, it is more likely that the sample was not fully magnetized. Therefore further experimental investigations, such as angle-resolved photoemission spectroscopy and magnetic circular dichroism would help to estimate this character. We also note that the predicted Cu and Mn magnetic moments are −0.41 μ_B, and 2.64 μ_B, while the experimental values are −0.75 and 2.59 μ_B, respectively (see Table 1). Therefore based on the calculation above, we further added the electron correlation on the Cu 3*d* orbit, that is GGA+$U_{f,d}$+SOC. Here the SOC is added on the Tb 4*f* state and *U* is added simultaneously on the Tb 4*f* and Cu 3*d* states with U_f=6.0 eV and U_d=5.0 eV. The calculated spin, orbit, and total magnetic moments are also listed in Table 1. Using this method, the calculated magnetic moments for Cu and Mn are −0.70 μ_B, and 2.64 μ_B, which are very close to the experimental values (−0.75 and 2.59 μ_B, respectively, in [12]). This actually indicates that our U_d=5.0 eV for Cu 3*d* is proper.

3.3. Magnetic coupling between Tb and Cu/Mn

In order to investigate how Tb couples with Cu/Mn, the site- and partial-density of states in AF2 magnetic state for the spin-up channel is plotted in Fig. 3(a) (the whole spin-down channel is more localized). It is observed from Fig. 3(a), that a large part of the occupied Tb 4*f* states is now situated at the highest O 2*p* states, making the top of the spin-up valence band a mixed Tb 4*f*–O2*p*–Cu3*d*/Mn3*d* character, where hybridization is evident from the relatively broad 4*f* PDOS. On more detailed analysis of Fig. 3(a), one can clearly see the peak around −2.75 eV corresponding to the localized Tb 4*f* electron. On the other hand, the small Tb 4*f* DOS in the range −2.0∼−1.4 eV corresponds to hybridized 4*f* states. A further indication of this Tb 4*f*–O2*p*–Cu3*d*/Mn3*d* interaction can be observed from the similarity in the positions of the peak at −1.5 eV where the spin-down Tb 4*f* DOS has a very similar character. Fig. 3(b) shows the electron density within the interval −2.0∼−1.4 eV (spin-up plus spin-down), which clearly shows the magnetic coupling between the three magnetic sublattices by way of O 2*p* orbitals. This similar analysis has been used to understand the magnetic coupling effect within PrO_2 [27].

4. Conclusion

In conclusion, using the accurate density-functional method a systematic computations of $TbCu_3Mn_4O_{12}$ at GGA, GGA+U_f, GGA+SOC, GGA+U_f+SOC, GGA+$U_{f,d}$ under lower symmetry crystal structure, and GGA+$U_{f,d}$+SOC levels have been carried out. Our

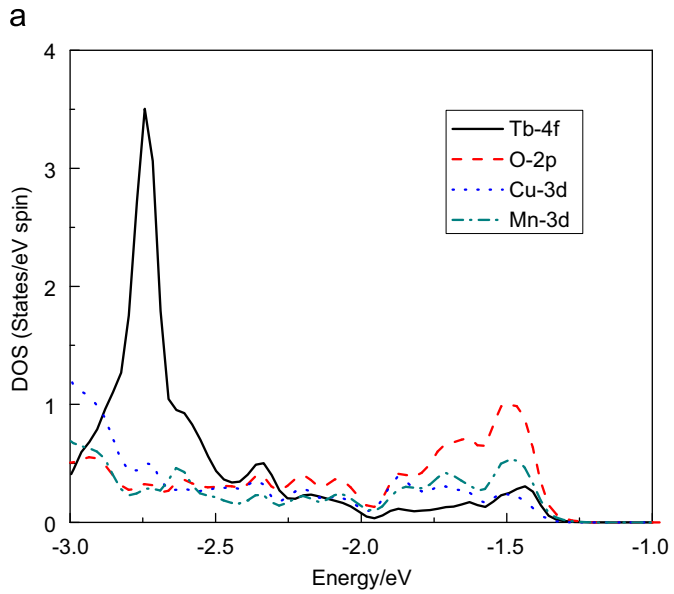

Fig. 3. (Color online) (a) GGA+$U_{d,f}$ +SOC spin-up DOS of $TbCu_3Mn_4O_{12}$ in the AF2 magnetic state for U_{eff}=6.0 eV of Tb 4*f* and U_{eff}=5.0 eV of Cu 3*d*. (b) Electron density corresponding to the electronic states from the energy range extending from −2.75 to −1.4 eV. The red and blue colors correspond to positive and negative values, respectively.

magnetic calculation reveals that the most stable magnetic state exists when Tb is ferromagnetically/antiferromagnetically coupled with Cu/Mn where Cu and Mn are antiferromagnetically coupled to each other. Our calculated electronic results also indicate that $TbCu_3Mn_4O_{12}$ is a half-metallic three-sublattice ferrimagnetic system with a large magnetic anisotropy, and its half-metallic nature can only be correctly described when electron correlation is considered on Tb 4*f* states. It is believed that the magnetic coupling between Tb and Cu/Mn is by way of 4*f*–2*p*–3*d*. Furthermore, in order to obtain correct magnetic moments, one needs to consider the electron correlation on Cu 3*d* states.

Acknowledgments

This work was partially supported by the National Natural Science Foundation of China through Grants no. 20831004, 20671088, and 20601026, and by AFOSR FA9550-06-1-0317. The authors would like to thank the reviewer for his/her constructive comments.

References

[1] M. Imada, A. Fujimor, Y. Tokura, Rev. Mod. Phys. 70 (1998) 1039.
[2] A.S. Nicola, F. Manfred, Science 391 (2005) 309.
[3] T. Todura, Colossal Magnetoresistive Oxides, Gordon and Breach, New York, 1999.
[4] W.E. Pickett, J.S. Moodera, Phys. Today 54 (2001) 39.
[5] Z. Zeng, M. Greenblatt, M.A. Subramanian, M. Croft, Phys. Rev. Lett. 82 (1999) 3164.
[6] H. Wu, Q. Zheng, X. Gong, Phys. Rev. B 61 (2000) 5217.
[7] I.O. Troyanchuk, L.S. Lobanovsky, N.V. Kasper, M. Hervieu, A. Maignan, C. Michel, H. Szymczak, A. Szewczyk, Phys. Rev. B 58 (1998) 14903.
[8] J. Sanchez-Benitez, J.A. Alonso, A. de Andres, M.J. Martinez-Lope, M.T. Casais, J.L. Martinez, J. Magn. Magn. Mater. 272 (2004) e1407.
[9] I.O. Troyanchuk, D.D. Khalyavin, M. Hervieu, A. Maignan, C. Michel, K. Petrowski, Phys. Status Solidi. A 169 (1998) R1.
[10] K. Schwarz, P. Blaha, Comput. Mater. Sci. 28 (2003) 259.
[11] X.J. Liu, H.P. Xiang, P. Chai, X.F. Hao, Z.J. Wu, J. Meng, J. Mater. Chem. 16 (2006) 4248.
[12] J. Sánchez-Benítez, J.A. Alonso, A. de Andrés, M.J. Martínez-Lope, J.L. Martínez, A. Muñoz, Chem. Mater. 17 (2005) 5070.
[13] A.A. Taskin, Y. Ando, Phys. Rev. Lett. 98 (2007) 207201.
[14] K.P. Belov, Phys. Usp. 39 (1996) 623.
[15] M. Pardavi-Horvath, J. Magn. Magn. Mater. 215–216 (2000) 171.
[16] P. Blaha, K.G. Schwarz, K.H. Madsen, D. Kvasnicka, J. Luitz WIEN2k, An Augmented Plane Wave+Local Orbitals Program for Calculating Crystal Properties, Karlheinz Schwarz, Techn. Universität Wien, Austria, 2001, ISBN3-9501031-1-2.
[17] J.P. Perdew, K. Burke, M. Ernzerhof, Phys. Rev. Lett. 77 (1996) 3865.
[18] J. Kuneš, P. Novák, M. Diviš, P.M. Oppeneer, Phys. Rev. B 63 (2001) 205111.
[19] D.D. Koelling, B.N. Harmon, J. Phys. C 10 (1977) 3107.
[20] A.H. MacDonald, W.E. Pickett, D.D. Koelling, J. Phys. C 13 (1980) 2675.
[21] A. Lichtenstein, V. Anisimov, J. Zaanen, Phys. Rev. B 52 (1995) R5467.
[22] V. Anisimov, F. Aryasetiawan, A. Lichtenstein, J. Phys.: Condens. Matter 9 (1997) 767.
[23] A. Petukhov, I. Mazin, L. Chioncel, A. Lichtenstein, Phys. Rev. B 67 (2003) 153106.
[24] R. Weht, W.E. Pickett, Phys. Rev. B 65 (2001) 014415.
[25] A.A. Taskin, Y. Ando, Phys. Rev. Lett. 98 (2007) 207201.
[26] P. Larson, W.R.L. Lambrecht, Phys. Rev. B. 75 (2007) 045114.
[27] F. Tran, J. Schweifer, P. Blaha, K. Schwarz, P. Novák, Phys. Rev. B 77 (2008) 085123.